Reaction Kinetics, Mechanisms and Catalysis (2022) 135:2735–2747
https://doi.org/10.1007/s11144-022-02288-6

# Photocatalytic mechanisms reactions of gallium doped $TiO_2$ thin films synthesized by sol gel (spin coating) in the degradation of methylene blue (MB) dye under sunlight irradiation

**Radhia Messemeche[1] · Youcef Benkhetta[1] · Abdallah Attaf[1] · Hanane Saidi[1] · Mohamed Salah Aida[2] · Okba Ben khetta[1]**

Received: 31 July 2022 / Accepted: 23 August 2022 / Published online: 29 August 2022
© Akadémiai Kiadó, Budapest, Hungary 2022

## Abstract

Thin films of pure $TiO_2$ and $Ti_{1-x}Ga_xO_2$ were prepared by the sol–gel method. The photocatalytic activity is tested by the degradation of the methylene blue (MB) dye under solar irradiation. Different methods are used in the characterization of materials and are X-ray diffraction, UV–visible. The results obtained show that the $Ti_{1-x}Ga_xO_2$ samples exhibit an anatase phase. The grain size has decreased. The degradation of methylene blue indicates that the photocatalytic activity of $Ti_{1-x}Ga_xO_2$ was significantly higher than that of pure $TiO_2$. The indication of photocatalytic efficiency could be effectively improved by gallium doping. The increase of oxygen vacancy amount and the realignment of the band gap resulting in the effect of Ga may be responsible for the enhancement of the photocatalytic activity. It found that the optimal photodegradation rate of 94% at t = 180 min at the doping concentration is 4%.

**Keywords** Thin films · $Ti_{1-x}Ga_xO_2$ · Sol Gel (spin coating) · Photocatalytic activity · Sunlight · Environmental pollution

## Introduction

Photocatalysis has become a new and important topic because it can completely degrade organic pollutants into harmless inorganic substances (such as $CO_2$, $H_2O$, etc.) under moderate conditions [1–4]. $TiO_2$ photocatalyst has gained considerable

✉ Abdallah Attaf
ab_attaf@univ-biskra.dz

[1] Physics of Thin Films and Applications Laboratory, University of Biskra, 07000 Biskra, Algeria

[2] Department of Physics, Faculty of Sciences, King Abdulaziz University, Jeddah 21589, Saudi Arabia

interest [5–12]. Anatase $TiO_2$, which is treated promising, has been an attraction in the photocatalytic degradation of environmental pollutants $TiO_2$ is proved the most suitable photocatalysts for its non-toxicity [1]. While, anatase $TiO_2$ (Eg = 3.2 eV) which is treated as WBG (a wide band gap) semiconductor can just be activated under ultraviolet (UV) irradiation (λo = 387 nm), which occupies only about 5% of solar energy. So, they tried every effort to develop photocatalysts that need less energetic but more sufficiently visible light through band engineering of doping [4, 6].

The main objective of metal ions doping is band gap narrowing and shifting up valence band or shift down conduction band of intrinsic $TiO_2$, which creates shallow intermediate band levels into the forbidden band through substituting Ti atoms by dopants in $TiO_2$ lattice. The intermediate band levels would act as recombination centers, which decrease electron–hole recombination. This various single metal ions have been widely studied to address the optical limitation of $TiO_2$ materials. Including transition metals such as V [13–16], Cr [17–21], Mn [22], Fe [23], Co [24], Ni [25], Cu [26], Zn [27], Zr [14], Mo, Ru, Rh, Ag [28, 29], Pt, rare earth metals, such as Ce, Pr, Sm, Eu, Gd and Er, other metals such as Mg, Sr, Ba, Ca and Pb. A great deal of theoretical and experimental works have been focused on doping $TiO_2$ with single metal ions, the exploitation of $TiO_2$ with doping still has a profound perspective because the chemical states of doping ions determined by the fabrication method play a crucial role in the doping effect [30].

By reducing the magnitude of the energy band gap, photons of lower energy can be absorbed by the material as well as affecting the recombination rate. Doping generally results in a mixture of doped and non-doped elements in the semiconductor. Important aspects to keep in mind when doping the semiconductor is that the ground state should be lower than the $O_2/H_2O$ level and conduction band higher than the $H_2/H_2O$ level to enhance the generation of hydroxyl radicals and thereby the photocatalytic activity. Modification of energy band gap should also allow the mobility of excited electrons and electron-holes across the $TiO_2$ surface to be able to reach active sites [30].

Gallium has been considered to improve photocatalytic conduct compared to undoped $TiO_2$ [1, 31–33]. Ga-doping will induce oxygen vacancies gaps and build deficiencies near the conductive band in $TiO_2$, which function as electron traps and increase the isolation of electron–hole pairs created by photographs [1, 33, 34]. In addition, due to the estimated ionic radii of $Ga^{3+}$ (62 pm) and $Ti^{4+}$ (68 pm), it is trivial to dope $Ga^{3+}$ at $Ti^{4+}$ sites in $TiO_2$ lattice [1, 31–33]. The synthesis of Ga–$TiO_2$ thin film has been obtained by different techniques as per the peer-reviewed literature such as the sol–gel method [1, 31, 33]. A hydrothermal method [1, 31, 35], and laser pyrolysis [36–38].

In this paper, $Ti_{1-x}Ga_xO_2$ thin films with x = 0.00, 0.02, 0.04, 0.08, and 0.10, respectively, were prepared by sol–gel (spin coating) method. The aim of this work is role of $Ga^{3+}$ on the photocatalytic activity of $TiO_2$ was investigated to obtain a higher photodegradation rate.

## Experimental details

### Preparation of $Ti_{1-x}Ga_xO_2$ thin films

$Ti_{1-x}Ga_xO_2$ thin films with x = 0.00, 0.02, 0.04, 0.08, and 0.10, respectively, have been successfully synthesized by a modified sol–gel (spin-coating) process using HOLMARC Spin Coater. Sol–Gel method is considered a facile process for the fabrication of high-quality thin films of metal oxide materials. Starting solution with a concentration of 0.2 M which was prepared by dissolving 0.604 ml of titanium tetra iso-prop-oxide (Ti [OC-H $(CH_3)_2]_4$) as the solution, 10 ml of ethanol ($C_2H_5OH$)which was used as a solvent, 0.207 ml of acetylacetone ($CH_3CH$) as a catalyst and gallium nitrate: $Ga(NO_3)_3$ as a source of gallium doping. The mass of gallium nitrate changes from 0.01 g to 0.05 g. This solution is a transparent yellowish color and slightly viscous. Where the ratio of Titan Tetra (IV) isopropoxide and acetylacetone is 1:1. Sodalime glass plates ($2.5 \times 2.5 \times 0.15$ $cm^3$) are used as the substrates, which it was chemically cleaned. The mixture was further stirred for 3 h by heating at a temperature of 50 C. The mixture solution was deposited on glass substrates using a spin coating system. Then, it was injected onto the center of the glass substrate at a rotation speed of 4000 rpm for 30 s. After 30 s, the deposited films were dried at 250 °C for 10 min in a furnace to evaporate the organic solvent. This step was repeated five times. Finally, $TiO_2$ films were annealed for 2 h at 500 °C in the furnace.

### Photocatalytic decolorization of MB

The photocatalytic activities of the as-synthesized samples were evaluated by photo-decolorizing methyl blue (MB) aqueous solution with a concentration of 15 mg/l. In each experiment, 10 mL of the MB solution is taken. Followed by the addition of $TiO_2$ thin films. The MB solution and $TiO_2$ thin films were exposed to natural sunlight in Algeria's country. All experiments are investigated at the 9:00 am in the month of September for 4 h. The dye concentration was determined by taking the UV absorption spectra using Perkin Elmer Lambda 950 UV/VIS spectrophotometer, in the wavelength range of 290–1100 nm. The highest absorbance at 664 nm was recorded for MB.

### Characterization methods

The synthesized structural and optical properties of the synthesized $TiO_2$ films were characterized by different techniques. The structure of the films was acquired by X-ray diffractometer (XRD) spectra(Model: Bruker D8) using Cu $K_\alpha$ radiation ($\lambda = 1.5418$ Å) at the 2θ range of 10°– 90°, with the steps of 0.02°. Besides, Perkin Elmer Lambda 950 UV/VIS spectrometer using to determine

the optical properties of deposited thin film (film thickness, transmittance, gap energy) ranging from 290 to 1100 nm.

## Results and discussion

### Structural characteristics

The XRD results of $Ti_{1-x}Ga_xO_2$ (x = 0, 0.02, 0.04, 0.06, 0.08 and 0.10) thin films shows in Fig. 1. The XRD results confirmed that the Ga-doped $TiO_2$ exhibits the tetragonal crystal structure with a single anatase phase and are agreed with the standard [JCPDS 21–1271]. The diffraction peak is 2θ = 25.36 indicating preferential crystal growth along the plane (101) [39].

The crystallite size (D) of $Ti_{1-x}Ga_xO_2$ films was measured using Scherrer's formula [39]

$$D = \frac{0.9\lambda}{\beta cos\theta} \tag{1}$$

Fig. 2 shows the change of the crystallite size as a function of the gallium doping concentration. The crystallite size increases from 17.77 nm to 19.75 nm at

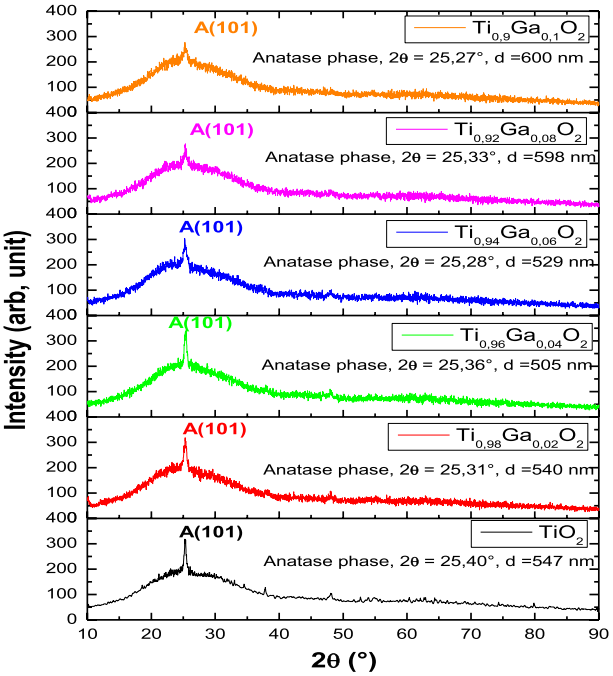


**Fig. 1** The XRD spectra of the $Ti_{1-x}Ga_xO_2$ thin films prepared by sol gel (spin coating) with x = 0, 0.02, 0.04, 0.06, 0.08 and 0.1 annealed at temperature of 500 °C for 2 h with C = 0.2 mol/L

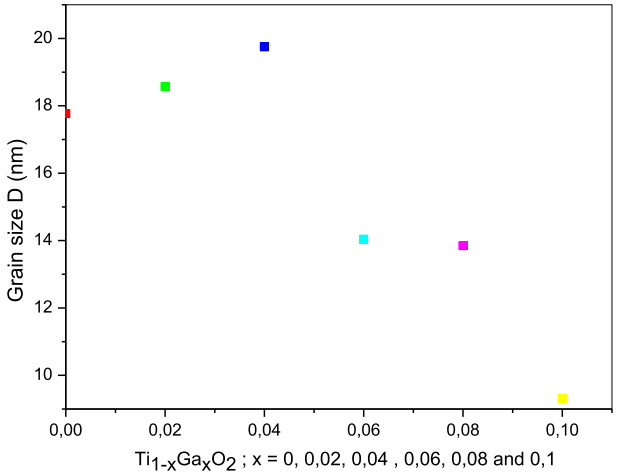


**Fig. 2** Crystallite size (D) of $Ti_{1-x}Ga_xO_2$ thin films prepared by sol gel (spin coating) annealed at temperature of 500 °C for 2 h with C = 0.2 mol/L with x = 0, 0.02, 0.04, 0.06, 0.08 and 0.1

x = 0.04. After that, it decreases to 9.30 nm with increasing doping concentration. The increase of crystallite size indicates an improvement of crystalline state of $Ti_{1-x}Ga_xO_2$ ($0 \leq x \leq 0.04$) thin films. This is results of $Ga^{3+}$ ions incorporation into $Ti^{3+}$ interstitials sites of $TiO_2$ lattice. At higher doping ($x > 0.04$), the effect of interstitials is compensated by the effect of substitution ($Ti^{4+}$ by $Ga^{+3}$) which leads to the decrease of crystallite size [40].

The dislocation density (δ) is defined as the length of dislocation lines per unit volume of the crystal has been calculated by using the Williamson and Smallman [39]:

$$\delta = \frac{1}{D^2} \tag{2}$$

Film thickness ***d*** has been calculated by using the Swanepoel method [39]:

**Table 1** Structural parameters of $Ti_{1-x}Ga_xO_2$thin films prepared by sol gel (spin coating)

| Samples $Ti_{1-x}Ga_xO_2$ | 2θ | D (nm) | $\delta \times 10^{16}$(line/m$^3$) | Thickness d (nm) |
|---|---|---|---|---|
| x = 0 | 25.40 | 17.77 | 5.62 | 547 |
| x = 0.02 | 25.31 | 18.57 | 5.38 | 540 |
| x = 0.04 | 25.36 | 19.75 | 5.06 | 505 |
| x = 0.06 | 25.28 | 14.04 | 7.12 | 529 |
| x = 0.08 | 25.33 | 13.85 | 7.22 | 598 |
| x = 0.1 | 25.27 | 9.30 | 10.6 | 600 |

$$d = \frac{\lambda_1 \lambda_2}{2\left(\lambda_1 n_2 - \lambda_2 n_1\right)} \tag{3}$$

The crystallite size, dislocation density (δ) and the thickness shows in the Table 1.

## Optical properties

The optical transmission spectra of $Ti_{1-x}Ga_xO_2$ thin films shows in Fig. 3. It can be seen, that the $Ti_{1-x}Ga_xO_2$ thin films have high transmittance at the samples of $TiO_2$, $Ti_{0.98}Ga_{0.02}O_2$, $Ti_{0.96}Ga_{0.04}O_2$, and $Ti_{0.94}Ga_{0.06}O_2$, where it reached 86%. This indicates that these samples have a good crystalline state and are consistent with the results obtained from DRX spectra.

After that, the transmittance decreases at $Ti_{0.92}Ga_{0.08}O_2$ and $Ti_{0.9}Ga_{0.1}O_2$. Whereas a higher concentration of Ga doping leads to a lower transmittance due to the interaction between the light and $Ga^{3+}$ ion. The appearance of interference fringe was observed in the samples $TiO_2$, $Ti_{0.98}Ga_{0.02}O_2$, $Ti_{0.96}Ga_{0.04}O_2$, and $Ti_{0.94}Ga_{0.06}O_2$. This indicates that the surface of the samples is smooth. As for other samples, the interference fringe did not appear which indicates that the surface of the samples is rough.

At high energy, absorption results from electronic transitions between wide states of band-to-band. Tauc law [39] usually describes it:

$$(\alpha h\nu)^n = A\left(h\nu - E_g\right) \tag{4}$$

Here $h\nu$ is the photon energy, $Eg$ is optical gap n and $A$ are constants, n characterizes the optical type of transition and takes the values 2 for allowed direct transitions or 1/2 for allowed indirect transitions).

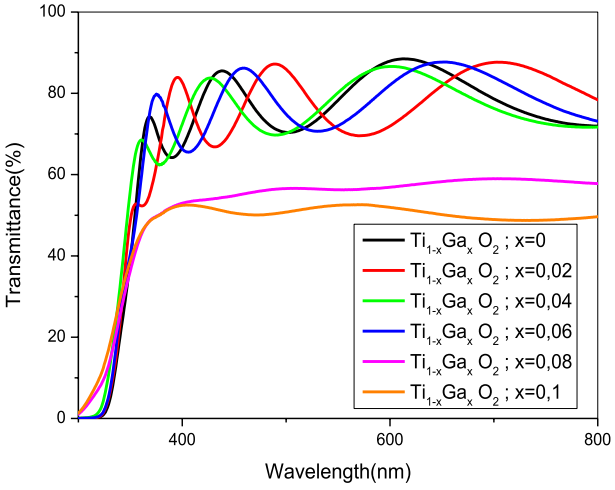


**Fig. 3** The optical transmission spectra of $Ti_{1-x}Ga_xO_2$ thin films deposited by sol gel (spin coating) annealed at temperature of 500 °C for 2 h with C = 0.2 mol/L; x = 0, 0.02, 0.04, 0.06, 0.08 and 0.1

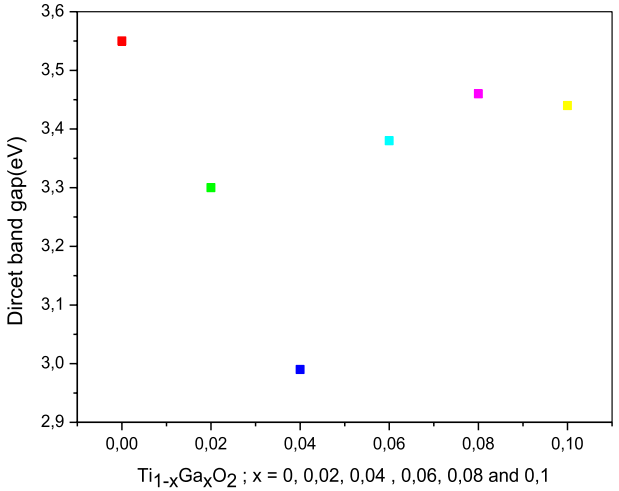


**Fig. 4** Direct band gap of $Ti_{1-x}Ga_xO_2$ thin film annealed at temperature of 500 °C for 2 h with C = 0.2 mol/L with x = 0, 0.02, 0.04, 0.06, 0.08 and 0.1

The direct band gab of $Ti_{1-x}Ga_xO_2$ film with different Ga doping concentrations shows in Fig. 4. It was observed that the direct band gab decreases with increasing the Ga doping concentration at the sample $Ti_{0.96}Ga_{0.04}O_2$and then increasing with increasing Ga doping concentration at the samples $Ti_{0.92}Ga_{0.08}O_2$ and $Ti_{0.9}Ga_{0.1}O_2$. In addition, it was observed that the direct band gab of Ga doped $TiO_2$ films less than of the pure $TiO_2$ films. This can be explained by the doping of $Ga^{3+}$ ions can form a $Ga^{3+}$ dopant level above the valence band (VB) of $TiO_2$. The indirect band gab of $Ti_{1-x}Ga_xO_2$ film with different Ga doping concentrations shows in Table 2.

**Table 2** Direct and indirect band gap of $Ti_{1-x}Ga_xO_2$ thin films prepared by sol gel (spin coating)

| Samples $Ti_{1-x}Ga_xO_2$ | Direct band gab (eV) | Indirect band gab (eV) |
|---|---|---|
| x = 0 | 3.55 | 3 |
| x = 0.02 | 3.30 | 2.96 |
| x = 0.04 | 2.99 | 2.76 |
| x = 0.06 | 3.38 | 3.24 |
| x = 0.08 | 3.46 | 3.33 |
| x = 0.1 | 3.44 | 3.29 |

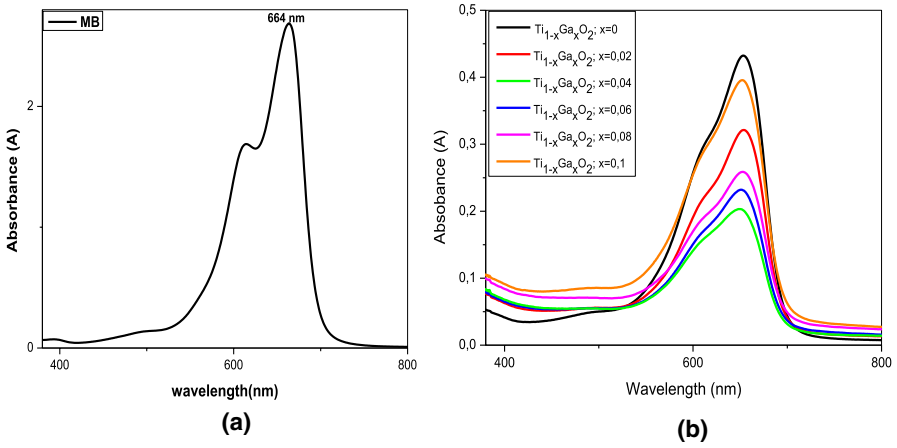


**Fig. 5** **a** UV–Vis **a**bsorption spectra of MB solution. **b** UV–Vis **a**bsorption spectra of MB solution with $C_{MB}=15$ mg/L after reacting with $Ti_{1-x}Ga_xO_2$ thin films (x = 0, 0.02, 0.04, 0.06, 0.08 and 0.1) for 4 h sunlight irradiation

## Photocatalytic activity studies

### Photocatalytic activity of $Ti_{1-x}Ga_xO_2$ films

Photocatalytic activity of $Ti_{1-x}Ga_xO_2$ films was evaluated by photodecomposition of MB dye in an aqueous solution of a concentration of $C_0=15$ mg/L as a model pollutant. Fig. 5b shows the absorption spectrum of MB solution catalyzed over thin films. It can be seen that the absorption intensity (A) of MB solutions containing Ga- doped thin films is less than that of non-doped. This indicates that the removal of MB dye solution is greater when using the activated slices, while it can be concluded that the Ga-doped $TiO_2$ thin films have an effective role in the effectiveness of photocatalysis.

The photocatalytic degradation rate (*PDR*) of thin films for the photocatalytic degradation of organic pollution dye solution was calculated with the formula [41].

$$PDR(\%) = \frac{A_0 - A_t}{A_0} \times 100 \tag{4}$$

Here $A_0$ is the absorbance of MB dye solution before the illumination and $A_t$ is the absorbance of MB dye after sunlight exposure time *t*.

The values of photodegradation rate variation of Ga doped concentration are shown in Fig. 6. After 4 h sunlight irradiation, about 95% of MB molecules are decolorized over the $Ti_{0.96}Ga_{0.04}O_2$thin film, while only 84%, 89.2%, 92.2%, 91.2% and 87.3% are decolorized over $TiO_2$, $Ti_{0.98}Ga_{0.02}O_2$, $Ti_{0.94}Ga_{0.06}O_2$, $Ti_{0.92}Ga_{0.08}O_2$, and $Ti_{0.9}Ga_{0.1}O_2$ thin films respectively. It was clearly seen that the photodegration rate is increased with Ga-doping concentration, getting more efficient at $Ti_{0.96}Ga_{0.04}O_2$ and then decreased gradually due to at a higher concentration the

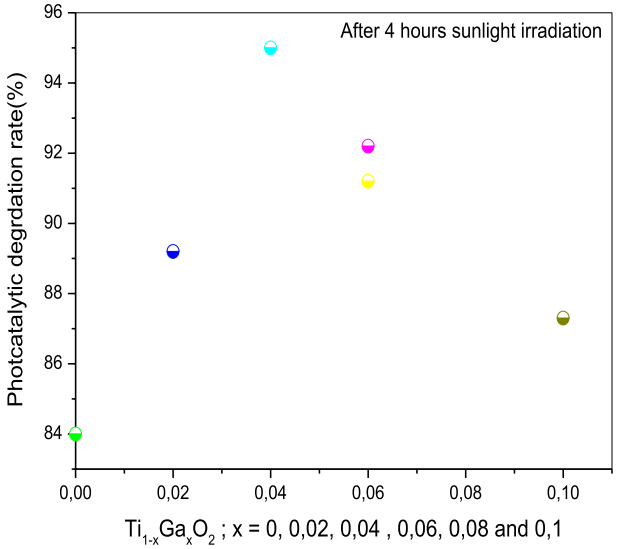


**Fig. 6** Photocatalytic degradation rate of MB solution after reacting with $Ti_{1-x}Ga_xO_2$ thin films with x = 0, 0.02, 0.04, 0.06, 0.08 and 0.1 for 4 h sunlight irradiation

distance between trapping sites decreases and thus increases the probability of recombination rate of the charge carriers [20]. Lin et al. [21, 42] and Mathews et al. [43].

## Mechanism of photocatalytic reaction

The possible mechanism for enhanced Photocatalytic activity of $Ti_{1-x}Ga_xO_2$ thin films is proposed as follows. Due to the Ga doping, the band edge shifted into the visible light, which would be favorable for the Photocatalytic activity under visible light. When the semiconductor Ga- $TiO_2$ doped thin films were exposed to suitable light, electrons (e−) are excited to the conductive band (CB) from the valance band (VB), which leads to generating electron (e−)/ (h+) hole pairs (Eq. 5) [43] The ionic radius of $Ga^{3+}$ (0.62 Å) being slightly lesser than the ionic radii of the $Ti^{4+}$ (0.68 Å) [17, 44, 45], it is possible for the $Ga^{3+}$ to substitute and occupy $Ti^{4+}$ sites. The DRX spectra found no significant difference of the 2θ on anatase plane (101) between pure $TiO_2$ and Ga-doped $TiO_2$ thin films, which also implies that $Ga^{3+}$ can easily enter into the lattice of $TiO_2$ and substitute for the $Ti^{4+}$ ion. As a result, the substitution of $Ga^{3+}$ to $Ti^{4+}$ ion could create a charge imbalance and then more $H_2O$/hydroxide ions would be adsorbed onto the surface of $TiO_2$ catalysts for charge balance. These adsorbed $H_2O$ or OH− ions on the surface could trap the surface holes and produce highly reactive hydroxide radicals (OH·). [46, 47] which could not only suppress the photo-induced electron–hole pair recombination rate, but also oxidize and adsorb more reactive substrates, and then improved its photocatalytic performance efficiently. The doped $Ga^{3+}$ions reduce the photoinduced electron–hole

pair recombination rate due to the energy level $Ga^{3+}/Ga^{4+}$. Photo-oxidation process (Eq. 6) above the VB of anatase $TiO_2$, develops charge carrier separation [43, 46]. The trapped surface holes in the photooxidation can migrate to the surface adsorbed hydroxyl ions to generate hydroxyl radicals (OH·) (Eq. 7).

$$Ti_{1-x}Ga_xO_2 + h\nu \rightarrow Ti_{1-x}Ga_xO_2 + \left(e^-_{CB} + h^+_{VB}\right) \tag{5}$$

$$Ga^{3+} + h^+_{VB} \rightarrow Ga^{4+} \tag{6}$$

$$Ga^{4+} + OH^-(Ads) \rightarrow Ga^{3+} + OH^{\cdot} \tag{7}$$

$Ga^{3+}$ traps the photoinduced electron to form $Ga^{2+}$ Eq. 8, and the trapped electrons transfer to the surface adsorbed $O_2$ (Eq. 9) or a neighboring $Ti^{4+}$ ions, and thus yield superoxide radicals ($O_2^{\cdot-}$) [46, 47]. The energy level of $Ga^{3+}/Ga^{2+}$ below the CB of anatase $TiO_2$ [24], supporting to enhance the charge carrier separation and resulting in the decline of the (e−)/(h+) pair recombination. The subsequent reactions Eqs. 7 and 9 demonstrated that $Ga^{3+}$ could act as electron–hole trapper [48, 49]. As a result, the doping of suitable $Ga^{3+}$ ions is favorable for the decrease of the photo induced e−/h+pairs recombination rate and favors the improvement of photocatalytic activity.

$$Ga^{3+} + e^-_{CB} \rightarrow Ga^{2+} \tag{8}$$

$$Ga^{2+} + O_2(ads) \rightarrow Ga^{3+} + O^{\cdot}_2 \tag{9}$$

However, at very high doping concentration, unfortunately $Ga^{3+}$ ions can performance as a charge carrier (photo induced electrons and holes) recombination centers (Eqs. 10 and 11), and due to decrease the distance between trapping sites at a high concentration of $Ga^{3+}$ ions and resulting in decline of the Photocatalytic activity.

$$Ga^{4+} + e^-_{CB} \rightarrow Ga^{3+} \tag{10}$$

$$Ga^{2+} + h^+_{VB} \rightarrow Ga^{3+} \tag{11}$$

## Conclusion

$Ti_{1-x}Ga_xO_2$ thin films were prepared by sol–gel (spin coating). The influence of the gallium doping concentration on the properties of $TiO_2$ was studied. The obtained results confirmed that the Ga-doped $TiO_2$ exhibits the tetragonal crystal structure with a single anatase phase. The grain size varied from 9.3 nm to 19.75 nm. The direct optical bandgap varied between 2.99 eV and 3.55 eV. It found that the optimum photodegradation rate of 94% at t = 180 min at doping concentration is 4%. It can be concluded, that the doping of galium ($0 \leq x \leq 0.04$) is narrowing the band

gap, which creates shallow intermediate band levels into the forbidden band through $Ga^{3+}$ ions incorporation into $Ti^{3+}$ interstitials sites of $TiO_2$ lattice. The intermediate band levels would decrease electron–hole recombination. The latter increase the photocatalytic activity.

## References


1. Mohamed HH, Fatimah AA (2021) Design of porous Ga doped TiO2 nanostructure for enhanced solar light photocatalytic applications. Mater Res Bull 133:111057
2. Bahnemann DW, Kholuiskaya SN, Dillert R, Kulak AI, Kokorin AI (2002) Photodestruction of dichloroacetic acid catalyzed by nano-sized $TiO_2$ particles. Appl Catal B 36:161–169
3. Mohamed H, Hammami I, Akhtar S, Youssef TE (2019) Highly efficient Cu-phthalocyanine-sensitized ZnO hollow spheres for photocatalytic and antimicrobial applications. Compos B Eng 176:1–9
4. Xu T, Liu X, Wang S, Li L (2019) Ferroelectric oxide nanocomposites with trimodal pore structure for high photocatalytic performance. Nano-Micro Lett 11:1–16
5. Choi W, Termin A, Hoffmann MR (2002) The role of metal ion dopants in quantum-sized $TiO_2$ correlation between photoreactivity and charge carrier recombination dynamics. J Phys Chem 98:13669–13679
6. Yan H, WangYao XM, Yao X (2013) Band structure design of semiconductors for enhanced photocatalytic activity: The case of $TiO_2$, progress in natural science. Mater Int 23:402–407
7. Chen X, Mao SS (2007) Titanium dioxide nanomaterials: synthesis, properties, modifications, and applications. Chem 107:2891–2959
8. Mohamed HH, Dillert R (2012) Bahnemann, $TiO_2$ nanoparticles as electron pools: Single- and multi-step electron transfer processes. J Photochem Photobiol A 245:9–17
9. Mohamed HH, Alomair NA, Alsanea AA, Ahtar S, Bahnemann DW (2019) ZnO porous graphite nanocomposite from waste for superior photocatalytic activity. Environ Sci Pollut 26:12288–12301
10. Mohamed HH, Alsanea AA (2020) $TiO_2$/carbon dots decorated reduced graphene oxide composites from waste car bumper and $TiO_2$ nanoparticles for photocatalytic applications. Arab J Chem 13:3082–3091
11. Mohamed HH, Hammami I, Baghdadi HA, Al-Jameel SS (2018) Multifunctional $TiO_2$ microspheres-rGO as highly active visible light photocatalyst and antimicrobial agent. Material Express 8:345–352
12. Mohamed HH, Alomair NA, Bahnemann DW (2019) Kinetic and mechanistic features on the reaction of stored $TiO_2$ electrons with Hg (II), Pb (II) and Ni (II) in aqueous suspension. Arab J Chem 12:5134–5141
13. Li L, Liu C, Liu Y (2009) Study on activities of vanadium (IV/V) doped $TiO_2$ (R) nanorods induced by UV and visible light. Mater Chem Phys 113:551–557
14. Zhou J, Takeuchi M, Ray AK, Anpo M, Zhao XS (2007) Enhancement of photocatalytic activity of P25 $TiO_2$ by vanadium-ion implantation under visible light irradiation. J Colloid Interface Sci 311:497–501
15. Wu JC, Chen C (2004) A visible-light response vanadium-doped titania nanocatalyst by sol– gel method. J Photochem Photobiol, A 163:509–515
16. Bhattacharyya K, Varma S, Tripathi AK, Tyagi AK (2010) Synthesis and photocatalytic activity of nano V-doped $TiO_2$ particles in MCM-41 under UV–visible irradiation. J Mater Res 25:125–133
17. Takeuchi M, Yamashita H, Matsuoka M, Anpo M, Hirao T, Itoh N, Iwamoto N (2000) Photocatalytic decomposition of NO under visible light irradiation on the Cr-ion-implanted $TiO_2$ thin film photocatalyst. Catal Lett 67:135–137
18. Sun B, Reddy EP, Smirniotis PG (2005) Effect of the $Cr^{6+}$ concentration in Cr-incorporated$TiO_2$-loaded MCM-41 catalysts for visible light photocatalysis. Appl Catal B 57:139–149
19. Zhu J, Deng Z, Chen F, Zhang J, Chen H, Anpo M, Huang J, Zhang L (2006) Hydrothermal doping method for preparation of Cr3+-$TiO_2$ photocatalysts with concentration gradient distribution of $Cr^{3+}$. Appl Catal B 62:329–335
20. Takaoka GH, Nose T, Kawashita M (2008) Photocatalytic properties of Cr-doped $TiO_2$ films prepared by oxygen cluster ion beam assisted deposition. Vacuum 83:679–682

21. Zhu H, Tao J, Dong X (2010) Preparation and photoelectrochemical activity of Cr-Doped $TiO_2$ nanorods with nanocavities. The Journal of Physical Chemistry C 114:2873–2879
22. Devi L, Kumar S, Murthy B, Kottam N (2009) Influence of $Mn^{2+}$ and $Mo^{6+}$ dopants on the phase transformations of $TiO_2$ lattice and its photo catalytic activity under solar illumination. Catalysis Commun 10:794–798
23. George S, Pokhrel S, Ji Z, Henderson BL, Xia T, Li L, Zink JI, Nel AE, Madler L (2011) Role of Fe doping in tuning the band gap of $TiO_2$ for the photo-oxidation-induced cytotoxicity paradigm. J Am Chem Soc 133:11270–11278
24. Barakat MA, Schaeffer H, Hayes G, Ismat-Shah S (2005) Photocatalytic degradation of 2-chlorophenol by Co-doped $TiO_2$ nanoparticles. Appl Catal B 57:23–30
25. Yu H, Li X, Zheng S, Xu W (2006) Photocatalytic activity of $TiO_2$ thin film non-uniformly doped by Ni. Mater Chem Phys 97:59–63
26. Colon G, Maicu M, Hidalgo MC, Navio JA (2006) Cu-doped $TiO_2$ systems with improved photocatalytic activity. Appl Catal B 67:41–51
27. Shao G, Deng Q, Wan L, Guo M, Xia X, Gao Y (2010) Molecular design of $TiO_2$ for giganticred shift via sublattice substitution. J Nanosci Nanotechnol 10:1–5
28. Zhang F, Cheng Z, Kang L, Cui L, Liu W, Xu X, Hou G, Yang H (2015) A novel preparation of Ag-doped $TiO_2$ nanofibers with enhanced stability of photocatalytic activity. RSC Adv 5:32088–32091
29. Gupta K, Singh RP, Pandey A, Anjana P (2013) Photocatalytic antibacterial performance of $TiO_2$ and Ag-doped $TiO_2$ against *S. aureus. P. aeruginosa* and *E. coli*. Beilstein J Nanotechnol 4:345–351
30. R.Car, G.Ertl, H.J.Freund, H.Lüth, M.A. Rocca, (2015) Defects at Oxide Surfaces. Springer Series in Surface Sciences
31. Chae J, Lee J, Jeong JH, Kang M (2009) Hydrogen production from photo splitting of water using the Ga-incorporated TiO2s prepared by a solvothermal method and their characteristics.B. Korean Chem 30:302–308
32. Chae J, Kim DY, Kim S, Kang M (2010) Photovoltaic efficiency on dye-sensitized solar cells (DSSC) assembled using Ga-incorporated $TiO_2$ materials. J Ind Eng Chem 16:906–911
33. Umare SS, Charanpahari A, Sasikala R (2013) Enhanced visible light photocatalytic activity of Ga, N and S codoped $TiO_2$ for degradation of azo dye. Mater Chem Phys 140:529–534
34. Ozaki H, Fujimoto N, Iwamoto S, Inoue M (2007) Photocatalytic activities of NH3- treated titanias modified with other elements. Appl Catal B 70:431–436
35. Depero LE, Marino A, Allieri B, Bontempi E, Sangaletti L, Casale C, Notaro M (2000) Morphology and microstructural properties of $TiO_2$ nanopowders doped with trivalent Al and Ga cations. J Mater Res 15:2080–2086
36. Bonini N, Carotta MC, Chiorino A, Guidi V, Malagù C, Martinelli G, Sacerdoti M (2000) Doping of a nanostructured titania thick film: structural and electrical investigations. Sens Actuators B 68:274–280
37. Deng Q, Han X, Gao Y, Shao G (2012) Remarkable optical red shift and extremely high optical absorption coefficient of V-Ga co-doped $TiO_2$. J Appl Phys 112:013523
38. Lee DK, Yoo HI (2008) Electrical conductivity and oxygen nonstoichiometry of acceptor (Ga)-doped titania. Phys Chem Chem Phys 10:6890–6898
39. Messemeche R, Saidi H, Attaf A, Benkhetta Y, Chala S, Nouadji R, Azizi R (2020) Elaboration and characterization of nano-crystalline layers of transparent titanium dioxide (Anatase-$TiO_2$) deposited by a sol-gel (spin coating) process. J Surfaces Interfaces 19:100482
40. Khatun N, Tiwari S, Vinod CP, Tseng CM, Liu SW, Biring S, Sen S (2018) Role of oxygen vacancies and interstitials on structural phase transition, grain growth, and optical properties of Ga doped $TiO_2$. J Appl Phys 123:245702
41. Khairy M, Zakaria W (2014) Effect of metal-doping of $TiO_2$ nanoparticles on their photocatalytic activities toward removal of organic dyes. Egypt J Pet 23:419–426
42. Czoska AM, Livraghi S, Chiesa M, Giamello E, Agnoli S, Granozzi G, Finazzi E (2008) The nature of defects in fluorine-doped $TiO_2$. J Phys Chem C 112:8951–8956
43. Komaraiah D, Eppa Radha J, Sivakumar MVR, Reddy RS (2019) Structural, optical properties and photocatalytic activity of $Fe^{3+}$ doped $TiO_2$ thin films deposited by sol-gel spin coating. Surfaces Interfaces 17:100368
44. Kim DH, Lee KS, Kim Y-S, Chung Y-C, Kim S-J (2006) Photocatalytic activity of Ni 8 wt%-doped $TiO_2$ photocatalyst synthesized by mechanical alloying under visible light. J Am Ceram Soc 89:515–518

45. Ortega Y, Lamiel-Garcia O, Hevia DF, Tosoni S, Oviedo J, San-Miguel MA, Illas F (2013) Theoretical study of the fluorine doped anatase surfaces. Surf Sci 618:154–158
46. Peng F, Cai LF, Yu H, Wang HJ, Yang J (2008) Synthesis and characterization of substitutional and interstitial nitrogen-doped titanium dioxides with visible light photocatalytic activity. J Solid State Chem 181:130–136
47. George S, Pokhrel S, Ji Z, Henderson BL, Xia T, Li L, Zink JI, Nel AE (2011) Role of Fe doping in tuning the band gap of $TiO_2$ for the photo-oxidation-induced cytotoxicity paradigm. J Am Chem Soc 133:11270–11278
48. Zhang XW, Lei LC (2008) One-step preparation of visible-light responsive Fe-$TiO_2$ coating photocatalysts by MOCVD. Mater Lett 62:895–897
49. Liu M, Qiu XQ, Miyauchi M, Hashimoto K (2013) Energy-level matching of Fe(III) ions grafted at surface and doped in bulk for efficient visible-light photocatalysts. J Am Chem Soc 135:10064–10072

**Publisher's Note** Springer Nature remains neutral with regard to jurisdictional claims in published maps and institutional affiliations.

Springer Nature or its licensor holds exclusive rights to this article under a publishing agreement with the author(s) or other rightsholder(s); author self-archiving of the accepted manuscript version of this article is solely governed by the terms of such publishing agreement and applicable law.